Blocking Losses On An Optical Communications Link

Bruce Moision, Sabino Piazzolla
Jet Propulsion Laboratory
California Institute of Technology
4800 Oak Grove Drive, Pasadena, CA 91109
bruce.moision,sabino.piazzolla@jpl.nasa.gov

***Abstract*—Many photon-counting photo-detectors have the property that they become inoperative for some time after detection event. We say the detector is *blocked* during this time. Blocking produces losses when using the detector as a photon-counter to detect a communications signal. In this paper, we characterize blocking losses for single detectors and for arrays of detectors. For arrays, we discuss conditions under which the output may be approximated as a Poisson point process, and provide a simple approximation to the blocking loss. We show how to extend the analysis to arrays of non-uniformly illuminated arrays and provide numerical methods to accurately predict count rates for detectors with exponential recovery from the blocked state.**

I. Introduction

Many photon-counting photo-detectors have the property that they become inoperative for some time after detection event. We say the detector is *blocked* during this time. When used to detect a communications signal, blocking leads to losses relative to an ideal detector, which may be measured as a reduction in the communications rate for a given received signal power, or a increase in the signal power required to support the same communications rate In this paper, we characterize blocking losses for single detectors and for arrays of detectors.

Throughout we assume the communications signal is intensity modulated, and received by an array of photon-counting photo-detectors. For the purpose of this analysis, we assume the detectors are ideal, in that they produce a signal that allows one to reproduce the arrival times of electrons, produced either as photo-electrons or from dark noise, exactly. For single detectors, we illustrate the performance of the maximum-likelihood(ML) receiver in blocking, as well as a *maximum-count*(MC) receiver, that, when receiving a pulse-position-modulated(PPM) signal, selects the symbol corresponding to the slot with the largest electron count. We show that whereas the MC receiver saturates at high count rates, the ML receiver may not. We numerically compute the loss in capacity, symbol-error-rate (SER), and count-rate. We show that the capacity and symbol-error-rate losses track, whereas the count-rate loss does not, generally, reflect the SER or capacity loss, as the slot-statistics at the detector output are no longer Poisson. We show that the MC receiver loss may be accurately predicted for dead-times on the order of a slot, by using the exact statistics provided in [1].

Blocking may be mitigated by spreading the signal intensity over an array of detectors, reducing the count rate on any one detector. We discuss conditions under which the sum of the arrayed detectors may be approximated as a Poisson point process, and provide a simple approximation to the blocking loss as a function of the probability that a detector is unblocked at a given time, essentially treating the blocking probability as a scaling of the detection efficiency. We show how to extend the analysis to arrays of non-uniformly illuminated arrays.

We also discuss incorporating a more accurate model of the blocking phenomenon, wherein the detector is blocked for some time, then has a recovery of its detection efficiency to the steady-state value. We illustrate in the Appendix how to accurately model the reduction in count rate for such a detector, and show that the additional loss due to the recovery time may be modeled by extending the blocking duration.

II. Channel Model

Suppose we are transmitting data over an optical link via intensity modulation with PPM of order M and slot width T_s. The signal, received on an array of K detectors, is modeled as a Poisson point process. The incident photon flux on the jth detector is

$$l_j(t) = l_b/K + l_s q_j M \sum_i u(t - T_s(x_i + iM)) \text{ photons/s}$$

where l_b and l_s are the cumulative background and signal rates over the entire array, q_j is fraction of the signal incident on the jth detector ($q_j \in [0,1]$, $\sum_j q_j = 1$), $u(t)$ is a unit pulse on $[0, T_s)$ ($u(t) = 1/T_s$ on $[0, T_s]$, and $u(t) = 0$ elsewhere), and $x_i \in \{0, 1, \ldots, M-1\}$ is the pulse position of the ith symbol. Section VI discusses distributions $\mathbf{q} = (q_1, \ldots, q_K)$ observed over a free-space channel with clear air turbulence. We assume the distribution $\mathbf{q}$ is constant. In general, the signal intensity pattern would be time-varying due to random changes in the optical phase front. However, in our cases of interest the coherence time of these variations is much longer than the symbol durations.

Let η be the detection efficiency, and l_d the detector dark rate. We assume a perfect detector/receiver, that reproduces the arrival time of each detected photo-electron or dark-current electron. In the remainder, we refer to all events at the output of the detector as electrons. Each detector is paralyzed, or

blocked, following the detection of an electron for a duration τ seconds[1] during which no electrons are produced. Due to the blocking, the output process is a self-excited point process. Let $N_j(t)$ denote the number of electrons produced by the jth detector on $[0,t)$, $\{w_1, w_2, \ldots, w_{N_j(t)}\}$ their ordered arrival times ($w_i < w_{i+1}$), and

$$\nu_j(t) = \eta l_j(t) + l_d$$

the intensity function of the unblocked electron process (the intensity of electrons in the absence of blocking). Suppose we observe arrivals over an interval $[0,T]$. The detector output sample function density, conditioned on l_j is [2]

$$p(\{N_j(t), 0 \le t \le T\}|l_j) =$$

$$\begin{cases} \exp\left(-\int_0^T \nu_j(t)dt\right) & , N_j(T) = 0 \\ \prod_{i=1}^{N_j(T)} \nu_j(w_i) \exp\left(-\sum_{i=1}^{N_j(T)+1} \int_{w_{i-1}+\tau}^{w_i} \nu_j(t)dt\right) & , \text{ otherwise} \end{cases}$$

where, for notational convenience, we define $w_0 \stackrel{\text{def}}{=} -\tau$ and $w_{n+1} \stackrel{\text{def}}{=} T$.

The point processes produced by each detector are conditionally independent. Letting $\mathbf{N}(t) = (N_1(t), \ldots, N_K(t))$ and $\mathbf{l} = (l_1, \ldots, l_K)$, the joint statistics of the detected process are

$$P(\{\mathbf{N}(t), 0 \le t \le T\}|\mathbf{l}) = \prod_{j=1}^{K} p(\{N_j(t), 0 \le t \le T\}|l_j)$$

III. Single Detector

We first consider reception of the signal with a single detector ($K = 1, q_1 = 1.0, N(t) = N_1(t)$). In the single detector case, we make the simplifying assumption in analysis that the detector is unblocked at the beginning of each PPM symbol. This effectively removes inter-symbol-interference (ISI) and allow us to find simple expressions for the maximum-likelihood(ML) SER and channel capacity, which would otherwise be complicated by the presence of ISI.

A. Symbol Error Rates

The ML symbol decision is given by

$$\hat{x}_{\text{ML}} = \arg \max_{x \in \{0,1,\ldots,M-1\}} p(\{N(t), 0 \le t \le MT_s\}|x)$$

where, to emphasize the symbol decision, we condition on the symbol position x, which completely specifies $l(t)$. Let n_j denote the number of counts in the jth slot (the interval $[(j-1)T_s, jT_s)$). In the absence of blocking, the collection of slot counts are a sufficient statistic for ML detection, and the ML decision reduces to selecting the slot with the maximum count. It's instructive to observe the behavior of this max-count(MC) receiver in the presence of blocking. Let

$$\hat{x}_{\text{MC}} = \arg \max_{x \in \{0,1,\ldots,M-1\}} n_x$$

[1]A more accurate model for some detectors is that the detection efficiency recovers exponentially. This will be treated in Section V-B1 and Appendix A.

Figure 1 illustrates the symbol error rate, $SER = P[\hat{x} \neq x]$, of the ML receiver, the MC receiver, and an unblocked receiver ($\tau = 0$), for the case $M = 16$, $\tau = 1.0$ ns, $l_b = 1.0e8$ photons/sec, $l_d = 0$, and $T_s = 2$ ns.

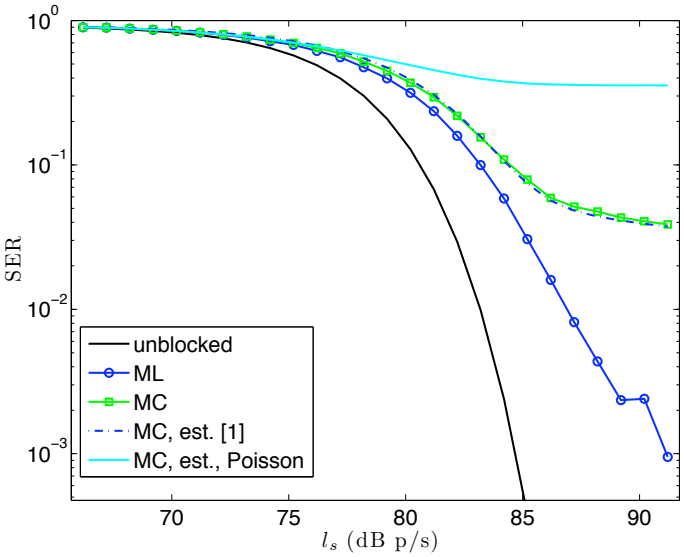

Fig. 1. Symbol Error Rates for a single blocked detector. Simulations with ML and MC symbol decisions. Also illustrated are two approximations to the MC error rate: using exact slot statistics from [1], and a Poisson approximation. $M = 16$, $T_s = 2.0$ ns, $\eta = 1.0$, $l_d = 0$, $\tau = 1.0$ ns, $l_b = 10^8$ photons/s

We also plot two analytic approximations to the MC receiver SER. The first approximation uses the true probability mass functions of noise and signal slots provided in [1]. However, it assumes the slot counts are independent. For τ small relative to MT_s, as in this example, the independence assumption is reasonable, and the approximation is accurate. The second approximation assumes the slot counts are Poisson distributed, using the simulated signal and noise slot mean count rates. We see that the Poisson assumption is inaccurate. Note that the MC receiver saturates at a SER corresponding to the probability that a noise slot has a count equal to the maximum achievable signal slot count. The ML receiver, which is able to extract information from the arrival times in a slot, and not just the total count, shows no such saturation.

B. Capacity

The capacity of the channel (assuming the receiver has access to all detection event times) with a input drawn uniformly on $\{1, \ldots, M\}$ is given by [3]

$$C_{\text{PPM}} = \frac{1}{MT_s} E_{X,N_t}\left[\log_2 \frac{\exp(L(N(t)|X))}{\frac{1}{M}\sum_j \exp(L(N(t)|x=j))}\right] \text{ bits/s}$$

where $E_{X,N(t)}$ is an expectation over X and $N(t)$, and $L(N(t)|x) = \log p(N(t)|x)$. Figure 2 illustrates the capacity, evaluated numerically, as a function of l_s for the operating point illustrated in Figure 1. At large signal power, the capacity approaches the same limit as for the unblocked case,

$\log_2(M)/(MT_s)$. We can see this intuitively, since there is information conveyed in the inter-arrival-times, not only the slot counts, and the inter-arrival-times in a signal slot can be reduced by increasing the signal power.

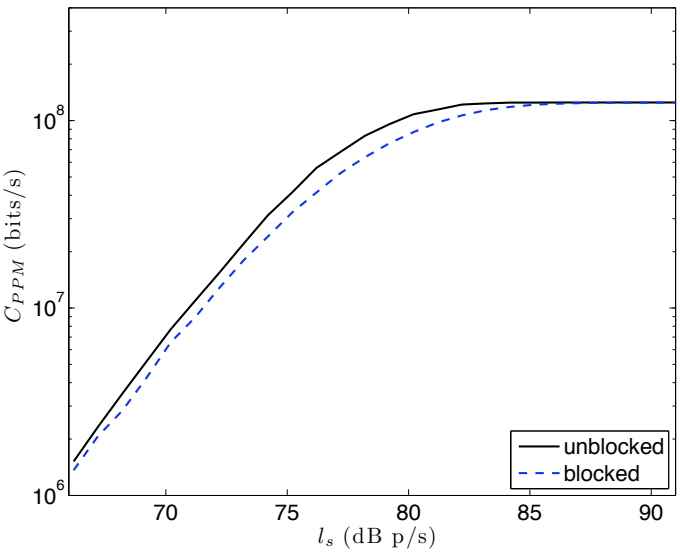

Fig. 2. Blocked and Unblocked Capacities. $T_s = 2.0$ ns, $M = 16$, $\tau = 1.0$ ns, $\eta = 1.0$, $l_d = 0$, $l_b = 10^8$ p/s

C. Assessing Losses

Figure 3 illustrates several measures of the blocking loss for the case $T_s = 2$ ns, $\tau = 1$ ns, $l_d = 0$ and $l_b = 10^8$ photons/s. The loss in SER and capacity are the dB increase in l_s required to bring about the same SER or capacity as an unblocked detector. The loss in count rate is the difference between the unblocked signal rate, ηl_s, and the signal count rate at the detector output.

We see that the ML SER loss tracks well with the capacity loss. We expect that the capacity of the MC receiver would also track with the MC SER loss. The plots show that the ML receiver achieves a gain over the MC receiver (a lower signal power to achieve the same SER), although the gains diminish at low SER. The SER and count-rate losses grow unbounded at high signal power, whereas, as noted earlier, the capacity loss goes to zero at high power (a discontinuity in the limit).

How should the loss be assessed? The relevant loss is the increase in signal power required to transmit data at a specified error rate. We assume the information bits are encoded with a power efficient error-correction-code prior to being mapped to PPM symbols. Suppose the systems use codes of rate $1/2$. The relevant operating point then corresponds to a capacity $\log_2(M)/(2MT_s)$. Modern ECCs can achieve acceptably low error rates at signal powers ≈ 2 dB in excess of capacity (accounting for implementation losses). In cases where the capacity is difficult to measure, we take the loss corresponding to a target uncoded SER of $0.2(M-1)/(M/2)$, corresponding to information bit-error-rate (post-decoding) of $\approx 10^{-6}$. Utilizing the SER as a measure has the advantage that the SER may be estimated directly via simulation when analytical expressions are intractable.

For example, in Figure 3, the relevant range of l_s, from Figure 2, would be ≈ 78 dB. Here the loss in using an MC receiver, for example, is less pronounced.

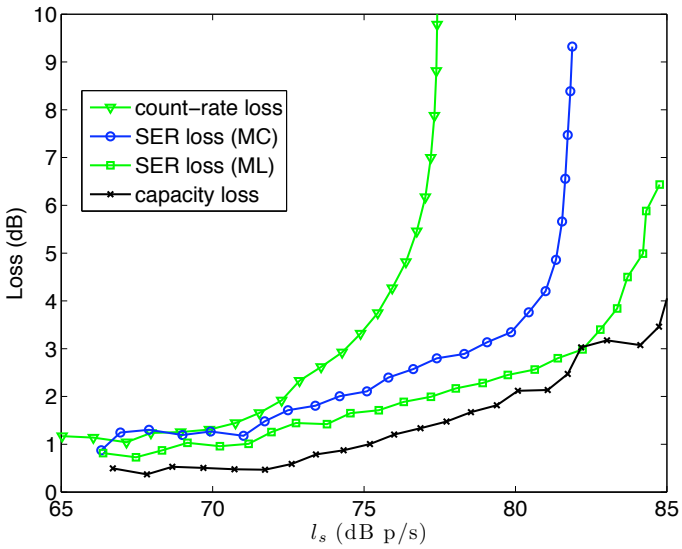

Fig. 3. Blocking Losses measured in terms of count rate, MC SER, ML SER and Capacity (ML). $M = 16$, $T_s = 2.0$ ns, $l_d = 0$, $l_b = 10^8$ photons/s, $\tau = 1.0$ ns

IV. Multiple Detectors

In most practical cases, the signal will be focused on an array of detectors. This enables pointing and tracking algorithms and spatial filtering. For detectors with blocking, spreading the signal over many detectors lowers the signal flux per detector, mitigating blocking (presuming blocking is dominated by the signal).

Figure 4 illustrates an example of a uniformly-illuminated ($q_i = 1/K$ for all i) array with $K = 16$, $l_b = 1.6 \times 10^8$ p/s, $l_d = 10^3$ e/s, $\tau = 48T_s$, $M = 8$, $T_s = 1.0$ ns. The MC SER and unblocked SER are illustrated. In these simulations, we no longer assume the detector is initially unblocked. Also illustrated are several approximations to the SER. These are described in the following section.

V. Predicting Blocking Loss

In this section we derive methods to predict the blocking loss for an MC receiver. The first subsection uses a prior result on the slot statistics in the presence of blocking. In cases where the slot counts are reasonably modeled as independent, the individual slot statistics are sufficient to estimate the blocking loss. The remaining subsections develop an approximate analysis for cases when the summed process may be modeled as a Poisson point process (and, hence, the slot statistics are well modeled as independent and Poisson). The loss may then be determined by scaling the electron rates. For this case, we derive a simple expression for the loss by approximating the capacity loss due to the rate reduction.

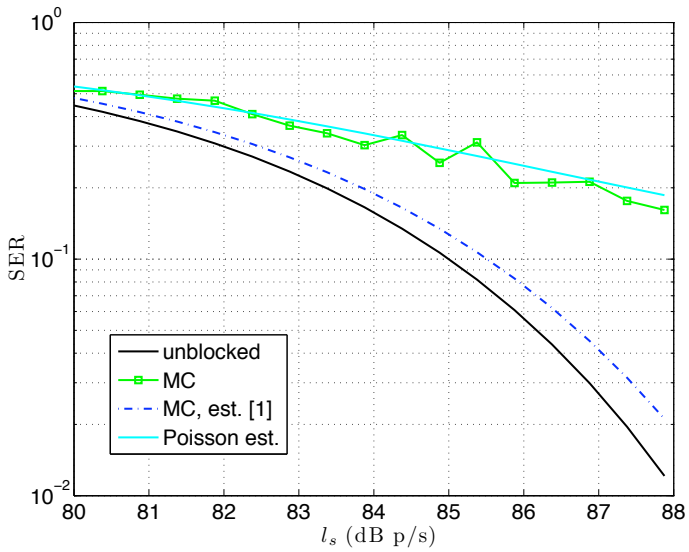

Fig. 4. Symbol Error Rates in Blocking with Uniform Illumination

A. Non-Poisson Statistics

Slot statistics in the presence of blocking are derived in [1]. That analysis may be extended to arrays of detectors as follows. Let $n_i^{(j)}$ be the number of counts in the ith slot of the jth detector, $p_{0,j}(k) = P(n_i^{(j)} = k | x \neq i)$ and $p_{1,j}(k) = P(n_i^{(j)} = k | x = i)$ the probability mass functions of a noise and signal slot, respectively, where x is the pulse position. These mass functions, under the approximation that every slot is preceded by a non-pulsed slot, were derived in [1]. Let $n_i = \sum_{j=1}^{K} n_i^{(j)}$, the summed count. Since the arrival processes are independent, we have

$$p_0(k) \stackrel{\text{def}}{=} P(n_i = k | x \neq i) = \underset{j=1}{\overset{K}{*}} p_{0,j}(k) \tag{1}$$

$$p_1(k) \stackrel{\text{def}}{=} P(n_i = k | x = i) = \underset{j=1}{\overset{K}{*}} p_{1,j}(k) \tag{2}$$

where $*$ denotes convolution.

Using the exact slot statistics, and assuming independent slot counts, provides accurate estimates of the MC receiver performance when the blocking duration is on the order of the slot duration, as illustrated in Figure 1 for a single detector (and, later, in Figures 8 and 11 for multiple detectors). However, the independence assumption breaks down for long blocking durations, where the statistics would have to account for the memory in the system. In the following sections, we develop a Poisson approximation, which will prove to be accurate in many cases of interest.

B. Blocking Probability

Suppose the unblocked electron rate of the detector is a constant l, and divide time into intervals of δ seconds. We may approximate the evolution of the detector state with an $L = \tau/\delta$ state Markov chain, illustrated in Figure 5. State 0 is the unblocked state. In the unblocked state, with probability $q_0 = \exp(-\delta l)$, no photons are detected and the detector remains unblocked. If photons are detected, the detector transitions to the blocked state L, and remains blocked for $L\delta = \tau$ seconds. Let μ_0 denote the probability the detector is in the unblocked state. We have

$$\mu_0 = \frac{1}{1 + Lq_1} = \frac{1}{1 + \frac{\tau}{\delta}(1 - e^{-\delta l})}$$

and, in the limit of small δ,

$$\mu_0 = \frac{1}{1 + \tau l} \tag{3}$$

Adding memory to the modulation, via PPM, will increase the blocking probability [4]. Nonetheless, we may model the probability that the detector is blocked at some time t as a stationary μ_0.

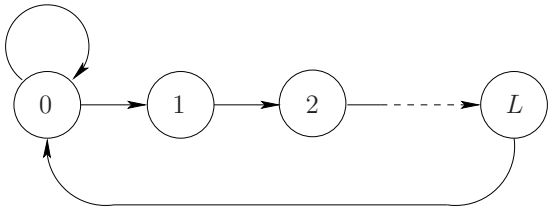

Fig. 5. Markov model of detector state

1) Adjustment for Exponential Recovery: A more accurate model of blocking for certain detectors is as a time-varying detection efficiency that goes to zero for a period of τ seconds after a detection event, and then rises exponentially, with time constant τ_b, back to its maximum value of η_0. That is, if the last detected event was at time s, the detection efficiency at time $t \geq s$ is

$$\eta(t) = \eta_0 \left(1 - \exp(-\max(0, t - s - \tau)/\tau_b)\right), t \geq s \tag{4}$$

An example with $\eta_0 = 0.5$, $\tau_b = 0.5T_s$ and $\tau = 0.2T_s$ is illustrated in Figure 6.

We may model the exponential recovery by extending the blocking duration such that the mean unblocked electrons produced over the duration of the recovery is preserved. That is, we take the blocking duration to be $\tau' = \tau + \tau_b$, so that, with $s = 0$,

$$\lim_{T \to \infty} \left(\eta_0 (T - \tau') - \int_0^T \eta(t) dt \right) = 0$$

C. Poisson Approximation: Sums of Point Processes

The sum of a collection of independent, uniformly sparse point processes converges in distribution to a Poisson point process [2, Theorem 5.2.3]. This suggests approximating the summed process as Poisson. But how accurate is this approximation for a finite number of processes?

One method to examine the accuracy is to consider the statistics of a count over a finite interval. Let Y_i be the count over an interval $\epsilon \leq \tau$ from detector i, and let $S_K = \sum_{i=1}^{K} Y_i$ be the sum of the counts over the interval. The sum S_K

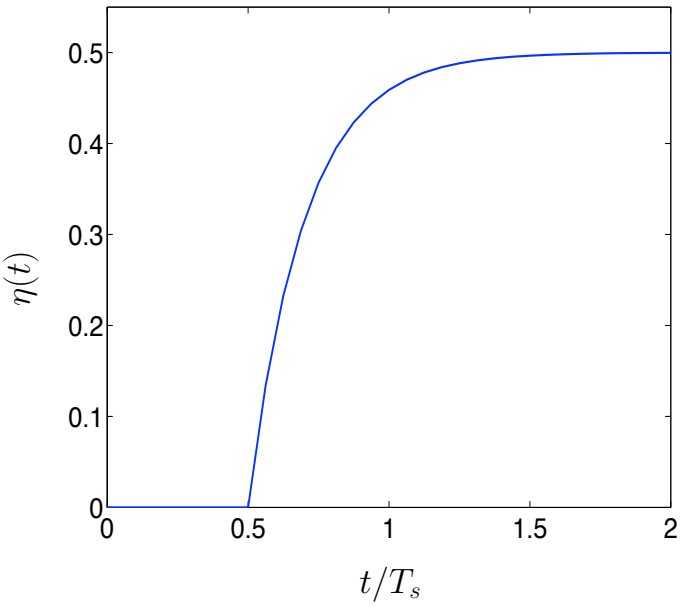

Fig. 6. Detection Efficiency–Recovery from a Detection Event at $s = 0$

converges in distribution to a Poisson random variable with mean $\mu = \sum_{i=1}^{K} p_i$ where $p_i = P[Y_i = 1]$ [5]. Suppose the unblocked electron process of the ith detector has a constant intensity l_i. One can show that

$$p_i = \frac{\epsilon l_i}{1 + \tau l_i}$$

The divergence between the distribution of S_K, P_{S_K}, and a Poisson random variable with mean μ, $Po(\mu)$, may be bounded as [5]

$$D(P_{S_K}||Po(\mu)) \leq \frac{1}{\mu} \sum_{i=1}^{K} \frac{p_i^3}{1 - p_i}$$

Suppose $l_1 = l_2 = \cdots = l_K$. Put $\epsilon = \tau$, the maximum duration over which the Y_i are binary. Then we have

$$D(P_{S_K}||Po(\mu)) \leq \frac{(\tau l_1)^2}{(1 + \tau l_1)}$$

As we would expect, the Poisson approximation becomes more accurate with decreasing mean counts per detector per dead-time–quadratically in τl_1 for small τl_1 (strictly speaking it also converges to a zero mean Poisson process for large τl_1). In particular, we are interested in how well a slot count is approximated as Poisson-distributed. Suppose $T_s \ll \tau$, put $\epsilon = T_s$, and use the approximation $(1+l_1(\tau - T_s)) \approx (1+l_1\tau)$. Then

$$D(P_{S_K}||Po(\mu)) \leq \left(\frac{T_s l_1}{1 + \tau l_1}\right)^2$$

Hence we may expect the Poisson approximation over a slot to be accurate even for large τl_1, so long as the mean counts per detector per slot time is small.

D. Poisson Approximation: Channel Capacity

In this section, motivated by the treatment in [6], we derive an approximation for the loss using the Poisson approximation described in Section V-C. Consider the channel in the absence of blocking, with mean signal rate ηl_s and mean noise rate $\eta l_b + K l_d$. One may bound the PPM capacity by the capacity of an intensity modulated channel with the same duty cycle, $1/M$, and infinite bandwidth. This bound is a good approximation to the PPM capacity, and losses computed based on it will prove to accurately reflect PPM losses. The capacity of the unblocked intensity modulated Poisson channel with duty cycle $1/M$ is given by [7]

$$C_u(l_s) = \eta l_s f(\rho) \text{ bits/s}$$

where

$$f(\rho) \stackrel{\text{def}}{=} \left(1 + \frac{1}{M\rho}\right) \log_2(1 + M\rho) - \left(1 + \frac{1}{\rho}\right) \log_2(1 + \rho)$$

and

$$\rho \stackrel{\text{def}}{=} \frac{\eta l_s}{\eta l_b + K l_d}$$

We will find it useful to use the approximation [8]

$$C_u(l_s) \approx \eta l_s g(\rho) \text{ bits/s}$$

where

$$g(\rho) \stackrel{\text{def}}{=} \frac{\log_2 M}{1 + \frac{1}{\rho} \frac{2 \log M}{M-1}}$$

In the presence of blocking, we may treat the probability that the detector is unblocked as a scaling of the detection efficiency, approximate the detected signal and noise rates as

$$l_s' = \eta l_s \sum_{i=1}^{K} \frac{q_i}{1 + \tau l_i} \tag{5}$$

$$l_b' = (\eta l_b / K + l_d) \sum_{i=1}^{K} \frac{1}{1 + \tau l_i} \tag{6}$$

where

$$l_i = \eta(q_i l_s + l_b/K) + l_d$$

and approximate the capacity as

$$C_b(l_s) \approx l_s' g(\rho')$$

where

$$\rho' = \rho \frac{\sum_{i=1}^{K} \frac{q_i}{1+\tau l_i}}{\sum_{i=1}^{K} \frac{1}{K} \frac{1}{1+\tau l_i}}$$

Suppose the illumination is uniform: $q_1 = q_2 = \cdots = q_K$, and, subsequently, $l_1 = l_2 = \cdots l_K$. Then $\rho' = \rho$ and the capacity loss is

$$\frac{C_b}{C_u} \approx \frac{1}{1 + \tau l_1} \stackrel{\text{def}}{=} \mu_0$$

Hence, at the same signal power, one can achieve a fraction $\approx \mu_0$ bits/s of the data rate that would be achievable with

an unblocked detector[2]. We may also state the loss in terms of the increase in signal power required to achieve the same capacity. Putting

$$C_u(l_s) \approx \eta l_s g(\rho) = \eta \tilde{l}_s \mu_0 g(\rho) \approx C_b(\tilde{l}_s)$$

and solving for l_s in terms of $\tilde{l}_s$ yields

$$l_s = \frac{\mu_0 \tilde{l}_s + \sqrt{(\mu_0 \tilde{l}_s)^2 + 4\mu_0 \psi(\tilde{l}_s + \psi)}}{2(1 + \psi/\tilde{l}_s)}$$

where

$$\psi = \frac{2 \log M(\eta l_b + K l_d)}{\eta(M-1)}$$

Hence the loss is

$$\text{loss} \stackrel{\text{def}}{=} \frac{\tilde{l}_s}{l_s} = \frac{2(\psi + \tilde{l}_s)}{\mu_0 \tilde{l}_s + \sqrt{(\mu_0 \tilde{l}_s)^2 + 4\mu_0 \psi(\tilde{l}_s + \psi)}} \qquad (7)$$

We may simplify the loss in the region where either the signal is dominant (high 'SNR') or the noise is dominant (low 'SNR'). Suppose $\psi \gg \tilde{l}_s$ (low SNR), then we have

$$\text{loss} \approx \frac{1}{\sqrt{\mu_0}}$$

Alternately, if $\psi \ll \tilde{l}_s$ (high SNR), we have

$$\text{loss} \approx \frac{1}{\mu_0}$$

We can also see this by noting that the capacity goes as $(l_s)^2/(l_s + l_b)$. To the extent that blocking is well modeled as a scaling of the detection efficiency by μ_0, at high SNR this yields a loss of μ_0, and at low SNR a loss of $\sqrt{\mu_0}$.

E. Poisson Approximation: Accuracy

Returning to Figure 4, on can accurately estimate the performance by assuming the detected point process is Poisson with signal and noise rates given by (5) and (6). Also illustrated is an estimate using (1) and (2) and assuming independent slot counts. That approximation is poor here, as the deadtime spans many slots.

Figure 7 illustrates an example of the more general model given by (4) with $K = 16$, $l_b = 1.6 \times 10^9$ p/s, $l_d = 10^3$ e/s, $T_s = 1$ ns, $M = 8$, $\tau = 8T_s$, $\tau_b = 16T_s$, and $\eta = 0.3$. Two estimates are illustrated, one using $\mu_0 = 1/(1 + \tau l)$ and one with the correction $\mu_0 = 1/(1 + (\tau + \tau_b)l)$. We see that the Poisson approximation with the correction term accurately predicts the loss due to blocking with exponential recovery.

However, if K is small, τl_1 and $T_s l_1$ are large, the Poisson approximation may be poor. Also, we note that if the background and dark noise are negligible, and the deadtime is on the order of a slot, then we have negligible loss, since with high probability only signal photons are detected, and a single detected signal photon is a sufficient statistic for ML symbol estimation.

[2]Note this pertains to the region of no bandwidth limit (arbitrarily small slot-widths), and doesn't contradict the asymptote in Figure 2 in the bandwidth constrained region

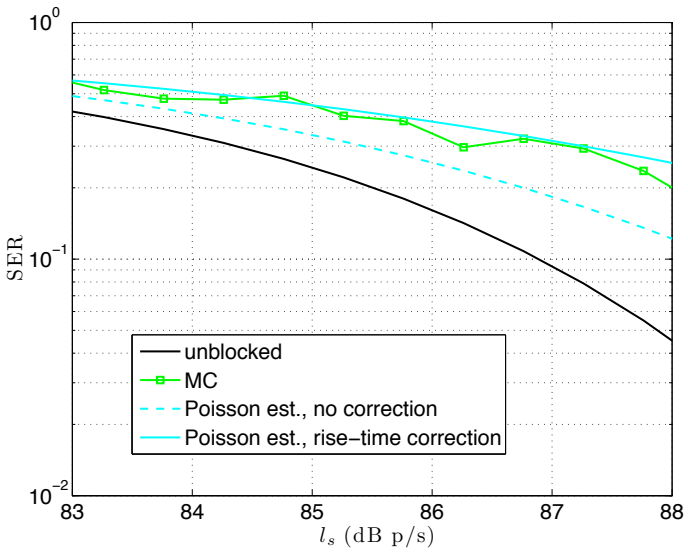

Fig. 7. Symbol Error Rates with Exponential Detection Efficiency Recovery Illustrating the Accuracy of the Rise-Time Correction

VI. Non-Uniform Intensity Patterns

In the general case, the signal flux on the collection of detectors will be non-uniform. In this section, we consider two non-uniform patterns: a diffraction-limited pattern, and a speckle pattern caused by atmospheric distortion of the signal.

With a non-uniform pattern, one can improve the performance by summing a subset of the detector outputs [9]. In fact, a weighted sum, in the absence of blocking, is a sufficient statistic for the ML receiver. We do not select a subset of the elements here, although the analysis could be extended to include that case. We assume the entire collection of detector outputs are summed, without weighting.

A. Diffraction-limited Intensity Pattern

Let $I(\boldsymbol{\rho})$ be the normalized signal field intensity in the focal plane at radial distance $\boldsymbol{\rho}$. Assume the incident signal is a normal plane wave. Then the intensity is an Airy function

$$I(\mathbf{r}) = \left(\frac{2J_1\left(\frac{\pi D \mathbf{r}}{\lambda F}\right)}{\frac{\pi D \mathbf{r}}{\lambda F}} \right)^2$$

where λ is the wavelength, D is the aperture diameter, F is the focal length, and J_1 is Bessel function of the first kind of order one. We will approximate this as Gaussian

$$I(\mathbf{r}) \approx \frac{1}{2\pi\sigma_g^2} \exp\left(\frac{-\mathbf{r}^2}{2\sigma_g^2}\right)$$

where $\sigma_g = 1.35\lambda F/(\pi D)$. Let the focal plane be divided into an array of K square pixels, where each pixel has width $2d$. The fraction of signal power integrated by the jth pixel is

$$q_j = \int_{\mathcal{A}_j} I(\mathbf{r}) d\mathbf{r}$$

where $\mathcal{A}_j$ is the area of the jth pixel. Figure 8 illustrates an example with $D = 20$ cm, $F = 1$ m, $K = 25$, $l_b = 6.25 \times 10^7$

p/s, $l_d = 10^3$ e/s, $T_s = 128$ ns, $\tau = 2T_s$, $M = 16$, $d = 5 \times 10^6$, and $\eta = 0.5$. Illustrated are the SER for the unblocked case, the blocked simulation, and three estimates of the blocked performance: one using the Poisson approximation with rates given by (5) and (6), one using (1) and (2) for the slot statistics, and one using (7), with μ_0 set by the detector with the maximum q_j. Since the blocking duration is moderate, the estimate from (1) and (2) is accurate. The Poisson approximation is less accurate, since, although K is large, the number of detectors with significant illumination by the signal is small. Finally, (7) accurately tracks the Poisson estimate, simply by choosing the detector with the maximum blockage.

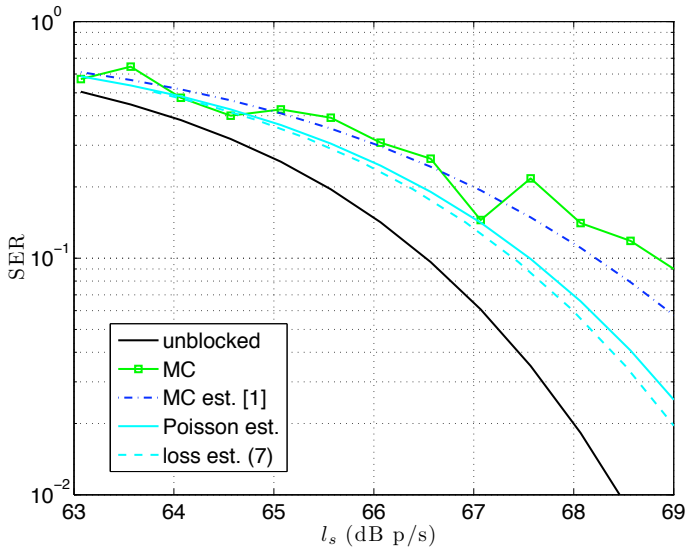

Fig. 8. Symbol Error Rates in Blocking with Airy-pattern Illumination

B. Focal Plane Signal Distribution in the Presence of Clear Air Turbulence (Speckled Intensity Patterns)

As a wave propagates through turbulent atmosphere, its phase is distorted. This phase distortion manifests itself at the focal plane of an imaging systems with a point spread function much larger than the diffraction limit. If the integration time of a pixellated detector or a CCD device at the focal plane is much less than the atmospheric coherence time, the distribution of light at the focal plane will be essentially speckled. That is, the energy content of the signal beam integrated over a slot time will be distributed at the focal plane in a number of speckles, each one of angular extension of a diffraction limited spot [10].

An accurate simulation of the speckled distribution at the receiver may be generated by using a Wave-Optics simulation, that simulates the propagation of the signal in a number of phase screens, and then images the distorted signal at the focal plane [11]. Wave-Optics simulations, however, are time consuming and problem specific (generalizing the results to problems with dissimilar initial condition is not straightforward).

However, using a heuristic approach, approximations, and some results from clear sky turbulence theory it is possible construct a satisfactory model. Consider a signal that is propagating in a turbulent atmosphere. The clear air turbulence and its effects on the beam propagation may be characterized by the atmospheric coherence length, r_0, given by

$$r_0 = \left(0.423k^2 \sec(\theta) \int C_n^2(h)dh\right)^{-3/5} (m)$$

where $k = 2\pi/\lambda$ is the wavenumber, θ is the path angle from zenith, and $C_n^2(h)$ is the refractive index structure coefficient along the vertical profile of the atmosphere at altitude h [12], which is a measure of the turbulence strength. To a first approximation, one can describe r_0 as the diameter of a disc over which the phase of a propagating wave at wavelength λ is approximately constant. The atmospheric coherence length varies during the day (smaller during daytime and larger during nighttime) and it is location dependent (larger in mountain top and smaller at sea level). For a good location, the atmospheric coherence length can assume values of tens of centimeters, while for a bad locations it is just few centimeters.

The effects of the clear air turbulence on the imaging system of a telescope are basically described by the ratio of the telescope diameter D to the atmospheric coherence length [10]. For $D/r_o < 3$ and for short-exposure, the spot size at the focal plane is approximately that of the diffraction limited spread function function. The variation of the angle of arrival (tilt) due to turbulence, will displace the location of the spot at focal plane. For short-exposure we define an integration time (or slot time) is less the atmosphere coherence time τ_{coh} approximately given by

$$\tau_{coh} \approx r_0/V$$

where V is the wind speed at ground, with τ_{coh} usually of the order of milliseconds [13]. For $D/r_o \gg 3$, and for exposure time much larger than τ_{coh} the full width half maximum of the point spread function at focal plane will angularly given by the astronomical seeing, defined as

$$S_e = \lambda/r_o$$

which is many time the diffraction limit of a typical telescope [12].

Finally, for $D/r_o \gg 3$ and for integration times less than τ_{coh}, the short-exposure point spread function is much larger than the diffraction limit (but less than that one given by the astronomical seeing). In this case the point spread function can be described by a Gaussian-like function [14]. For each realization, the centroid of this point spread function is still displaced over the focal plane by the tilt angle. The signal envelope at the focal plane will be described by a collection of speckles with the number of speckles approximately given by $(D/r_o)^2$, while for each realization the probability of speckle locations at the focal plane will be described by the short-exposure point spread function [10].

Our interest is the case where a pixellated detector is located in the focal plane. Here the overall response of the

system will depend on the number of pixels, the pixel pitch, and the number of speckles. If the number of the speckles is large relative to the number of illuminated pixels, the overall envelope of the pixel response will be similar to that described by the short-exposure point spread function sampled by detector pixels at the focal plane. If instead, the number of speckles is much less than the number of pixels covered by the short-exposure point spread function, than the overall response envelope will have a limited number of pixels illuminated by one or more speckles.

Figure 9 illustrates a speckle pattern for the case $D = 1.0$ m, $F = 1.5$ m, in presence of clear air turbulence with $r_0 = 10$ cm at $\lambda = 1550$ nm (the wavelength of operation). The theory predicts approximately $(D/r_0)^2 = 100$ speckles. At the focal plane there is an arrayed detector of 5 m pixel pitch . At this pitch, the pixels average multiple speckles, yielding the coarse distribution of photo-electron density per pixel illustrated in Figure 10 (illustrated is a $K = 81$ pixel array). Note that for intervals of time larger of the atmosphere coherence time, there will be a new realization at the focal plane with different distribution of the photo-electrons.

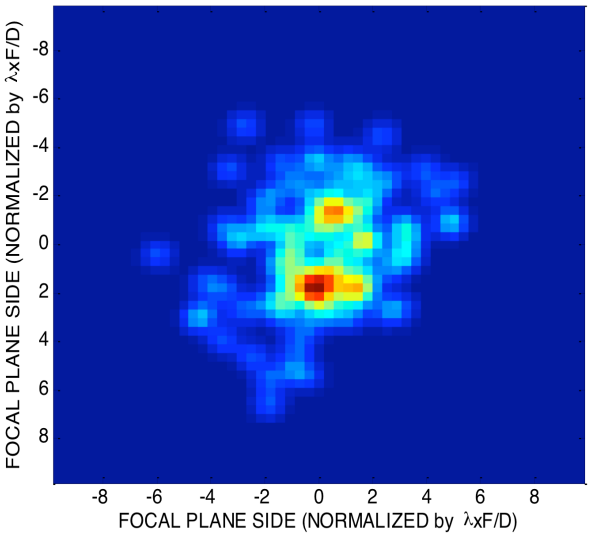

Fig. 9. Example Speckle Pattern: $D = 1.0$ m, $F = 1.5$ m, $r_0 = 10.0$ cm at $\lambda = 1550$ nm

Figure 11 illustrates performance for the speckle described in Figure 10 with $l_b = 8.0 \times 10^9$ p/s, $l_d = 10^3$ e/s, $T_s = 1.0$ ns, $\tau = 2T_s$, $M = 8$, $\eta = 1.0$, and $K = 81$. The same collection of performance curves described in Figure 8 are applied and illustrated here. With a moderate blocking duration, the estimate from (1) and (2) is roughly accurate, as is the Poisson. Similar to the Airy-pattern example, although K is large, the number of detectors with significant illumination by the signal is small (40% of the signal is collected by 4 detectors). Approximation (7) is indistinguishable from the Poisson estimate..

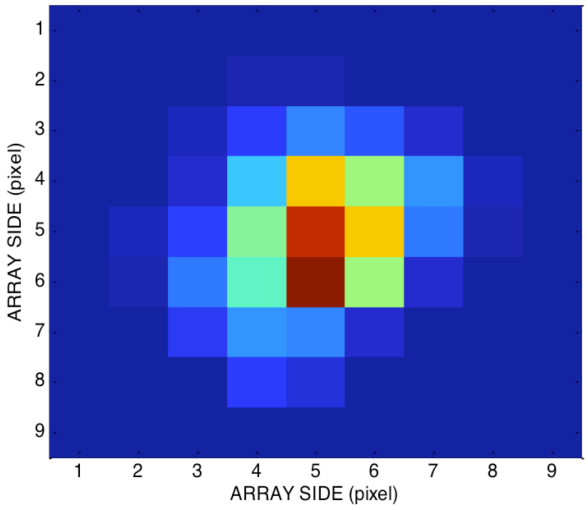

Fig. 10. Pixel intensity distribution from averaged speckle pattern: $2d = 5.0\mu$ m, $D = 1.0$ m, $F = 1.5$ m, $r_0 = 10.0$ cm at $\lambda = 1550$ nm

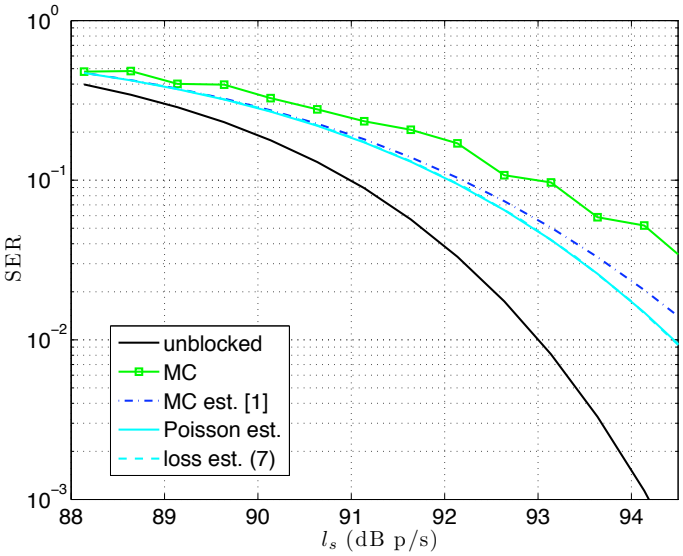

Fig. 11. Symbol Error Rates in Blocking with Speckled Illumination Pattern

VII. Conclusions

In this paper we have characterized losses on a photon-counting communications link due to detector blocking. We illustrated how to approximate the losses when the output is well characterized as Poisson, as well as numerical methods to evaluate the losses when it is not. The approximate losses allow a simple, accurate, approximation of blocking loss for most cases with a relatively large detector array and sparse event arrival rates.

Appendix

In this Appendix we provide a method to accurately estimate count rates at the detector output for the model of blocking with exponential recovery given by (4). The source is

memoryless Bernoulli, producing a pulsed slot, of duration T_s, with probability $1/M$, and a non-pulsed slot with probability $(M-1)/M$. Let n_s and n_b denote the mean un-blocked signal and noise electrons per slot, respectively.

Divide time into sub-slots of duration δ, where, for notational convenience, we assume δ divides τ, τ_b and T_s. The detector behavior may be accurately modeled with the Markov chain illustrated in Figure 12. On this graph, each transition corresponds to a step of duration δ. To simplify notation, throughout this section in evaluating $\eta(t)$ we set the last arrival to be $s = 0$. We approximate $\eta(t)$ as constant over each δ: state i corresponds to a detection efficiency of $\eta(i\delta)$ and state 1 denotes a detection event (and a reset of the detection efficiency). To restrict the number of states to be finite, we do not distinguish differences in the detection efficiency from the maximum when $\eta_0 - \eta(t) < \eta_0\epsilon$, for some $0 < \epsilon < 1$. That is, we put

$$B = \frac{\tau}{\delta}$$
$$U = B - \frac{\tau_b}{\delta}\lceil \ln(\epsilon) \rceil$$

B represents the blocking duration in sub-slots, and U the number of sub-slots required to return to the maximum detection efficiency.

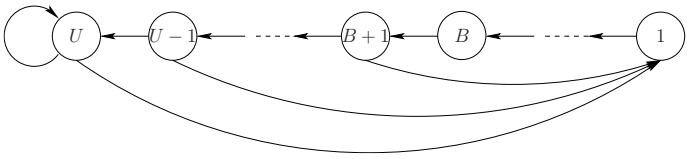

Fig. 12. Discrete-Time Markov Model of Detector

Due to the modulation, transition probabilities are constant for blocks of T_s/δ edges. In order to model this, we define transition matrices Q_0, Q_1 as follows. Let $S(n\delta) \in \{1, 2, \ldots, U\}$ denote the state at time $t = n\delta$ and $X \in \{0, 1\}$ the binary input (the slot is pulsed for $X = 1$ and non-pulsed for $X = 0$). Define the matrices Q_x, $x \in \{0, 1\}$, to have (i, j)-th element

$$[Q_x]_{i,j} = P(S(n\delta) = j | S((n-1)\delta) = i, X = x)$$
$$= \begin{cases} \exp(-(xn_s + n_b)\eta(i\delta)\delta/T_s) & , j = \max(U, i+1) \\ 1 - \exp(-(xn_s + n_b)\eta(i\delta)\delta/T_s) & , j = 1 \\ 0 & , \text{otherwise} \end{cases}$$

Q_1 and Q_0 are the *sub-slot* probability transition matrices for a pulsed and non-pulsed slot, respectively. The *slot* probability transition matrix is given by

$$[Q]_{i,j} = P(S(nT_s = j) | S((n-1)T_s = i)$$
$$= \frac{M-1}{M}[Q_0^{T_s/\delta}]_{i,j} + \frac{1}{M}[Q_1^{T_s/\delta}]_{i,j}$$

The slot probability matrix is aperiodic and irreducible. Hence the state probabilities approach the steady state values $P(S(n) = i) = [\mu]_i$ given by the (normalized) left eigenvector of Q.

$$\mu Q = \mu$$

A. Detected Count Rates

Let k denote the number of counts in a slot, and $k_i, i = 1, 2, \ldots, T_s/\delta$, denote the number of counts in sub-slot i (of duration δ). Assume that $\delta \leq \tau$. Then each sub-slot has at most one count, and the mean count in noise slot may be approximated (up to the discrete-time approximation) as

$$\begin{aligned} \tilde{n}_b &= E[k|x = 0] \\ &= \sum_{i=1}^{T_s/\delta} E[k_i|x = 0] \\ &\approx \sum_{i=1}^{T_s/\delta} P(S(i\delta = 1)|x = 0) \\ &= \left[\mu(Q_o + Q_0^2 + \ldots + Q_0^{T_s/\delta})\right]_1 \end{aligned} \quad (8)$$

(note that $\tilde{n_b}$ is the mean count in blocking, whereas n_b is the mean count if there were no blocking)where $[v]_1$ denotes element 1 of vector $[v]$ (corresponding here to state 1). Similarly, the mean counts in a pulsed slot may be approximated as

$$\begin{aligned} \tilde{n}_s + \tilde{n}_b &= E[k|x = 1] \\ &\approx (n_s \hat{+} n_b) = \left[\mu(Q_1 + Q_1^2 + \ldots + Q_1^{T_s/\delta})\right]_1 \end{aligned} \quad (9)$$

Figures 13 and 14 illustrate the count rates in a noise and signal slot from a simulation of the continuous-time model for the parameters corresponding to a single detector in Figure 7: $M = 8$, $T_s = 1$ ns, $l_b = 1.6 \times 10^9$ p/s (a rate of 10^8 per detector), $l_d = 10^3$ e/s, $\eta_0 = 0.3$, $\tau = 8T_s$, $\delta = T_s/4$, $\epsilon = 0.1$, and $\tau_b = 16T_s$. Also illustrated are the estimates (8), (9).

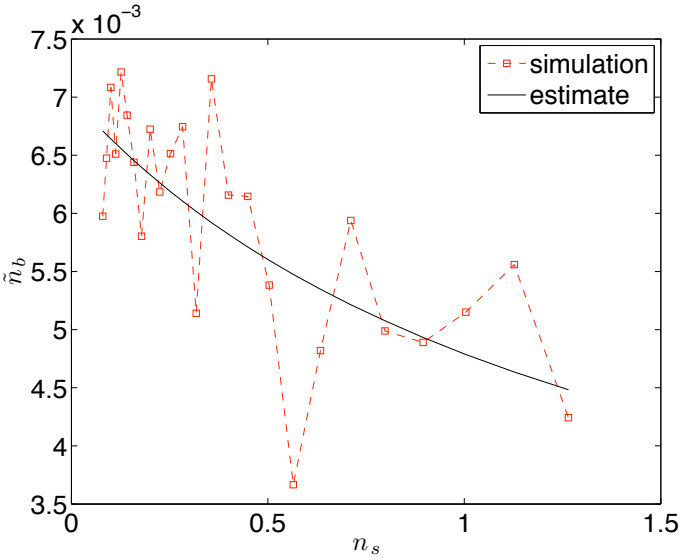

Fig. 13. Count rates in a noise slot: simulated and estimated

ACKNOWLEDGMENT

We would like to thank Baris Erkmen for helpful discussions on this material. The research described in this publication was supported by the JPL R&TD Task number R.11.023.026 and

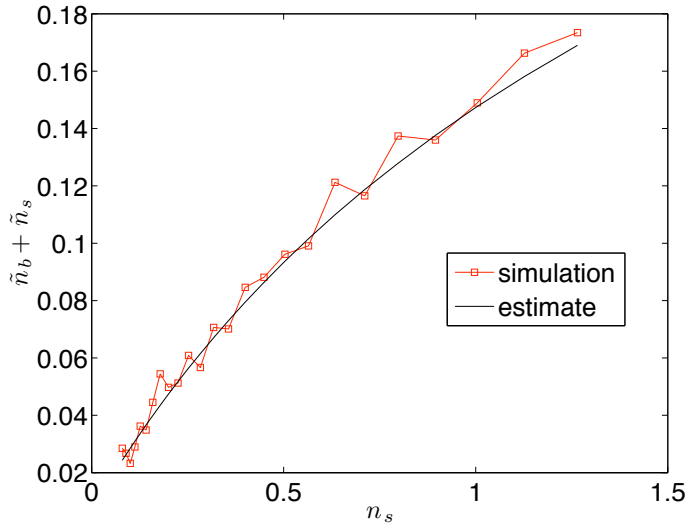

Fig. 14. Count rates in a signal slot: simulated and estimated

the DARPA InPho program under contract number JPL 97-15402, and was carried out by the Jet Propulsion Laboratory, California Institute of Technology, under a contract with the National Aeronautics and Space Administration.

REFERENCES

[1] C. C. Chen, "Effect of detector dead time on the performance of optical direct-detection communication links," *Telecommunications and Data Acquisition Progress Report*, vol. 42–93, pp. 146–154, January-March 1988.

[2] D. L. Snyder, *Random Point Processes*. Wiley, 1975.

[3] B. Moision and J. Hamkins, "Deep-space optical communications downlink budget: Modulation and Coding," *IPN Progress Report*, vol. 42-154, Aug. 2003.

[4] B. Moision, M. Srinivasan, and J. Hamkins, "The blocking probability of geiger-mode avalanche photo-diodes," in *SPIE* (B. Huang, R. W. Heymann, and C. C. Wang, eds.), vol. 5889, 2005.

[5] I. Kontoyiannis, P. Harremoës, and O. Johnson, "Entropy and the law of small numbers," *IEEE Transactions on Information Theory*, vol. 51, pp. 466–472, feb 2005.

[6] D. M. Boroson, "The communications penalty of refresh times in geiger-mode detectors," tech. rep., MIT-Lincoln Laboratory, April 2004.

[7] A. D. Wyner, "Capacity and error exponent for the direct detection photon channel–Part I," *IEEE Transactions on Information Theory*, vol. 34, pp. 1449–1461, Nov. 1988.

[8] B. Moision, "Capacity of the Poisson PPM channel: Some simple approximations and rules of thumb," tech. rep., Jet Propulsion Laboratory, August 2008.

[9] V. A. Vilnrotter and M. Srinivasan, "Adaptive detector arrays for optical communications receivers," *IEEE Transactions on Communications*, vol. 50, pp. 1091–1097, July 2002.

[10] J. W. Goodman, *Speckle Phenomena in Optics: Theory and Applications*. Roberts, 2007.

[11] D. M. Strong, E. P. Magee, and G. B. Lamont, "Implementation and test of wave optics code using parallel FFT algorithms," in *Proceedings of the SPIE*, no. 4167 in 34, 2001.

[12] L. C. Andrews, R. Phillips, and C. Y. Hopen, *Laser Beam Scintillation with Applications*. SPIE Press, 2001.

[13] M. Schoeck and E. J. Spillar, "Analysis of turbulent atmospheric layers with a wavefront sensor: testing the frozen flow hypothesis," in *SPIE* (R. K. Tyson and R. Q. Fugate, eds.), vol. 3762, pp. 225–236, 1999.

[14] L. C. Andrews, R. L. Phillips, R. J. Sasiela, and R. R. Parenti, "Strehl ratio and scintillation theory for uplink Gaussian-beam waves: beam wander effects," *Opt. Eng.*, no. 45, 2006.